CDF note 7081

# Measurement of $B^0$ Oscillations Using Same-Side Tagging in Semileptonic $B$ Decays

The CDF Collaboration
*URL http://www-cdf.fnal.gov*
(Dated: June 28, 2004)

We present a measurement of the $B^0$ mixing parameter $\Delta m_d$ measured in the partially reconstructed $B \to \ell D^{(*)}$ sample at the CDF experiment. Three final states are reconstructed with an integrated luminosity of about 245 $pb^{-1}$, which corresponds to a sample of over 115000 $B$ mesons. The initial $b$ flavor is determined by a Same-Side Tagging method developed in Run I. We find $\Delta m_d = (0.443 \pm 0.052\ (stat.) \pm 0.030\ (s.c.) \pm 0.012\ (syst.))ps^{-1}$, and tagging dilutions of $D_0 = (12.8 \pm 1.6\ (stat.) \pm 1.0\ (s.c.) \pm 0.6\ (syst.))\%$ and $D_+ = (28.3 \pm 1.3\ (stat.) \pm 1.1\ (s.c.) \pm 1.0\ (syst.))\%$. The first error is statistical, the second one comes from the sample composition, and the third one is the rest of the systematic uncertainties.

*Preliminary Results for Summer 2004 Conferences*

## I. INTRODUCTION

In this note we present a measurement of the $B^0$ mixing parameter $\Delta m_d$ using a $B \to \ell D^{(*)}$ sample obtained from the lepton+SVT trigger at the CDF experiment. The mixing and $CP$-violation parameters of $B$ mesons are currently the focus of much attention for pinning down the CKM matrix, and perhaps exposing new physics beyond the standard model. We are not in a position to make physically interesting measurements of parameters like $\Delta m_d$. But on the other hand it is crucially important that we measure well known parameters like $\Delta m_d$ to establish the credibility and capability of the CDF detector and the techniques which we wish to bring to bear on future tagging measurements, like $\Delta m_s$. This measurement of $\Delta m_d$ is thus an important step in that larger program.

As a contribution to this effort we have opted in this analysis to use similar approaches to the Run I $\Delta m_d$ mixing measurement using Same-Side Tagging (SST) in the partially reconstructed $B \to \ell D^{(*)}$ sample [1].

The sample selection and tagging are relatively straightforward ingredients to this analysis. The intricacy of this analysis centers around issues of the "sample composition". Our naive desire is to measure $B^0$ mixing through $B^0 \to \ell^+ \nu D^-$ decays (charge conjugates should always be assumed unless stated otherwise). One can proceed to reconstruct a sample of $\ell^+ D^-$, but this sample will in fact *not* be a pure $B^0$ sample. Because our ability to reconstruct final states is not perfect there is cross-talk between $B^+$ and $B^0$ decays. In particular a $B$ decay that proceeds through a $D^*$ or $D^{**}$ state and which subsequently decays to the $D$ ground state by the emission of one or more charged pions will be reconstructed as the wrong $B$ charge if an odd number of charged pions escapes the reconstruction. The $D^{*+} \to D^0 \pi^+$ is a good state to reconstruct, but the "soft" $\pi^+$ will often have a low $p_T$ which results in a significant reconstruction inefficiency feeding the $B^+ \leftrightarrow B^0$ cross talk. The situation is even worse for the $D^{**}$ which includes very broad states that are essentially impossible to identify, as well as non-resonant $B^+ \to \ell^+ \nu D^0 \pi^-$ decays. These cross-talk effects are not huge, but nor are they negligible.

The CDF detector is described in detail in [2].

## II. DATA SAMPLE & EVENT SELECTION

This analysis is based on an integrated luminosity of about 245 pb$^{-1}$ collected with the CDFII detector between March 2002 and January 2004. The data are collected with a trigger that requires an electron or muon with $P_T > 4$ GeV/c, and a displaced track from the primary vertex and $P_T >$ 2 GeV/c. The dataset selected above is called lepton+SVT trigger. Three $B$ meson final states are reconstructed in this analysis. These modes nominally correspond to the decays:

$$
\begin{aligned}
B^0 &\to \nu \ell^+ D^{*-}, \quad D^{*-} \to \overline{D}^0 \pi_*^-, \quad \overline{D}^0 \to K^+ \pi^-; \\
B^0 &\to \nu \ell^+ D^-, \quad D^- \to K^+ \pi^- \pi^-; \\
B^+ &\to \nu \ell^+ \overline{D}^0 \quad \overline{D}^0 \to K^+ \pi^-.
\end{aligned}
$$

The issue of the sample detailed composition is discussed later and remains so far hidden in the qualifier 'nominal'.

A common set of tools has been developed in order to reconstruct semileptonic $B$ decays. The lepton selection consists of confirmation of the electron and muon trigger tracks. $D$ meson candidates are selected in a loose mass window around the nominal PDG value [3]. At least one track of the $D$ candidate has to be a SVT track, the resulting $\chi^2$ in the $r - \varphi$ plane, $\chi^2_{r,\varphi}$, of the $D$ meson fit is required to be less than 40 and the two-dimensional decay length with respect to the primary vertex, $L_{xy}(D \to P.V.)$, has to be greater than 0.04 cm in order to reject non-$B$ decays. Once both lepton and $D$ meson are defined, $B$ candidates ($\equiv \ \ell + D$) are selected if the lepton and $D$ system has a mass lower than 5 GeV/c$^2$ and the error in the $ct(B)$ less than 0.04 cm, which removes poorly reconstructed events. A set of final requirements is differently applied for each channel. $B \to l^+ D^{*-} X$ candidates are selected if 0.1435 GeV/c$^2$ $< m_{D^{*-}} - m_{D^0} <$ 0.1475 GeV/c$^2$ and $P_T(\pi_s) > 0.4$ GeV/$c$. $B \to l^+ D^- X$ candidates are selected if $\frac{L_{xy}}{\sigma_{L_{xy}}}(\overline{D}^+ \to P.V.) > 10$, the $B$ vertex probability fit is greater than 0.01% and $ct(D^+)$ lies between $-0.01$ cm and 0.15 cm. Finally, $B \rightarrow l^+\overline{D}^0 X$ are required to have $\frac{L_{xy}}{\sigma_{L_{xy}}}(\overline{D}^0 \rightarrow P.V.) > 5$, $B$ vertex probability fit has to be greater than 0.01% and $ct(\overline{D}^0)$ must be between $-0.01$ cm and 0.10 cm. In order to minimize the "cross-talk" between $B^0$ and $B^+$ decays we remove as many of the $D^*$ mesons that contribute to the $D^0$ sample as we can identify. We do not accept any candidate which is compatible with $B \rightarrow l^+ D^{*-} X (D^{*-}$, where the soft pion momentum cut is not applied. Due to the incomplete reconstruction of the $B$ decays, the $B$ mass is not possible to fully reconstruct. Instead, the $D$ mass distribution is used to compute the yield for each channel.

The overall number of signal events, $\frac{S}{\sqrt{S+B}}$ and $\frac{S}{B}$ for all channels are shown in Table I. The results of these $B$ selections are shown in Figure 1. We use these events for the mixing analysis.

| Channel | Yield | $\frac{S}{B}$ | $\frac{S}{\sqrt{S+B}}$ |
|---|---|---|---|
| $B \rightarrow l^+ D^{*-} X (D^{*-} \rightarrow \overline{D}^0 \pi_*^-,\ \overline{D}^0 \rightarrow K^+\pi^-)$ | 9737 $\pm$ 113 | 13.5 | 95 |
| $B \rightarrow l^+ D^- X (D^- \rightarrow K^+\pi^-\pi^-)$ | 35951 $\pm$ 411 | 1.3 | 142 |
| $B \rightarrow l^+ \overline{D}^0 X (\overline{D}^0 \rightarrow K^+\pi^-)$ | 69591 $\pm$ 379 | 3.3 | 230 |

TABLE I: Number of signal events, $S/B$ and $\frac{S}{\sqrt{S+B}}$ for each channel.

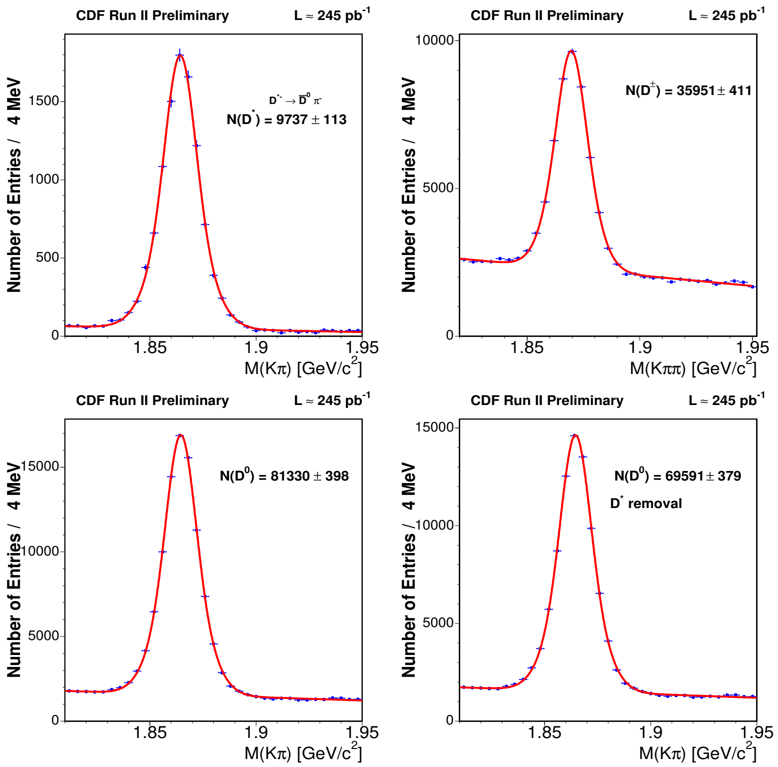


FIG. 1: Plots of the $D$ candidate masses of the three $B$ samples. The bottom left plot shows the selected $\overline{D}^0 \rightarrow K^+\pi^-$ mass distribution, and the right bottom plot shows the $\overline{D}^0$ sample after removing identified $D^{*-}$ candidates.

## III. SAME SIDE TAGGING ALGORITHM

The same-side flavor tagging technique (SST) was well established in Run I. It was originally pioneered in the $\ell D$ mixing analysis [1], and was the foundation for the $\sin 2\beta$ measurements [4]. The SST algorithm begins by considering all charged particles that pass through all stereo layers of the Central Outer Tracker, COT, i.e. require the track's exit radius from the COT is at least 130 cm; and that are within the $\eta$-$\phi$ cone of radius $\Delta R = 0.7$, being $\Delta R = \sqrt{\Delta\eta^2 + \Delta\phi^2}$, centered along the direction of the $B$ meson as approximated by the momentum sum from the partial $\ell D^{(*)}$ reconstruction. Tracks are required to be consistent with having originated from the fragmentation chain or the decay of a $B^{**}$ meson, *i.e.*, coming from the primary vertex of the $p\bar{p}$-interaction. This translates into the demand that tracks must have at least 3 SVX hits and $|d_0/\sigma_0| < 3$, where $d_0$ is the distance of closest approach of the track trajectory to the primary vertex when projected onto the plane transverse to the beam line ($r$-$\phi$ plane) and $\sigma_0$ is the estimated error on $d_0$. The central tracking chamber is known to have a lower reconstruction efficiency for positive tracks compared to negative ones at low $p_T$. To mostly suppress this undesired bias, all candidate tracks must have a $p_T$ above a threshold of 450 MeV/$c$.

## IV. SAMPLE COMPOSITION

This analysis uses three $\ell D^{(*)}$ samples, but as alluded to in the introduction, there are actually multiple decay paths that contribute to a given observed final state. A necessary complication is unraveling various types of cross-talk that contaminate a pure $B^0$ signal. The cross-talk between $B^0$ and $B^+$ decay chains that feed a given decay signature is the first concern. The various decay chains are mapped out in Figure 2. The path of a decay chain jumps up or down with the emission of a charged pion, and if it is undetected, one will mistake a $B^+$ for a $B^0$, or the reverse. The combined effect of the relative branching ratios at each decay step will determine the relative sizes of the various decay signatures. The relative branching fractions for $B$ decaying into $D$, $D^*$, and $D^{**}$ are respectively denoted by $f$, $f^*$, and $f^{**}$ in Figure 2. The rate at which $D^{**}$ mesons decay via $D^*$ mesons versus $D$ mesons is encoded in a parameter labeled $P_V$.

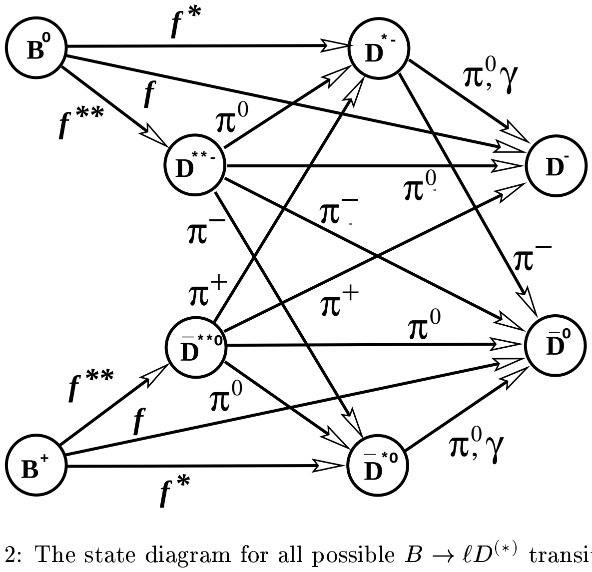


FIG. 2: The state diagram for all possible $B \to \ell D^{(*)}$ transitions.

The remaining branching ratios are well known. Note that the decay $D^{*-} \to \overline{D}^0\pi^-$ takes place, but its isospin partner $\overline{D}^{*0} \to \overline{D}^-\pi^+$ does *not*, thereby creating a significant asymmetry in the sample composition at the level of raw physics. Even more important to the sample composition than the differences in raw branching ratios is the elementary reality that our reconstruction is imperfect. In fact we do not even attempt to find $\pi_{**}$ tracks from $D^{**}$ decays, and when the $\pi_{**}$ is charged we suffer from cross-talk. Slightly more subtle is the loss of $\pi_*$ tracks from $D^*$ decays. We do attempt to find charged pions from $D^*$ decays, but this only occurs with some efficiency, $\epsilon(\pi_*)$. Lost charged pions from $D^{**}$ and $D^*$ decays are then the two sources of $B^0 \leftrightarrow B^+$ cross-talk.

Therefore, we must put all the sample composition parameters and the branching ratio inputs taken from the PDG [3] together to quantify the contributions of various decay chains for each decay signature. In addition we must apply a correction due to the different selection efficiencies of every decay chain. Furthermore the different lifetimes of $B^0$ abd $B^+$ mesons have to be considered. More explicit definitions and derivations of the algebraic implementation for expressing sample composition in terms of branching ratios and efficiencies can be found in Reference [1].

### A. $R^*$: Efficiency for Reconstructing $\pi_*$ tracks

The above inputs are all the principle ingredients needed to specify the sample composition for each decay chain, however, there is a remaining subtle component that comes into play, this is the efficiency for identifying the pion for $D^*$ reconstruction, $\epsilon(\pi_*)$. We use Monte Carlo simulation to determine the relative trigger and reconstruction efficiencies, with one exception. The pion from $D^*$ decays tends to be very soft and there is a significant chance that very low $p_T$ tracks will not be reconstructed or pass our COT quality cuts. Unlike the other efficiencies which are driven by geometrical or kinematic effects the $\pi_*$ efficiency is determined by basic characteristics of COT performance, something we do not trust the standard Monte Carlo simulations to describe reliably. We therefore rely upon our data sample to measure $\epsilon(\pi_*)$.

The basic concept behind measuring $\epsilon(\pi_*)$ is to look at the relative number of $\ell D^*$ candidates reconstructed relative to the total number of $\ell D^0$ candidates we find irrespective of whether or not the $\ell D$ is also part of the $\ell D^*$ sample, i.e., we measure the quantity

$$R^* \equiv \frac{N(\ell^+\overline{D}^0(\pi_*^\pm)) - N(\ell^+ D^0)}{N(\ell^+\overline{D}^0(\pi_*^\pm))}, \tag{1}$$

where "$\ell^+\overline{D}^0(\pi_*^\pm)$" signifies $\ell^+\overline{D}^0$ candidates *before* $D^{*-}$ removal. The delicate point is that the full $\ell D^0$ sample is an unspecified mixture of $B$ decays into $\ell D^0$ as well as decays into $\ell D^*$ where the $\pi_*$ may or may not have been identified. Fortunately the rest of the sample composition information, efficiencies and branching ratios, allows to predict the value of $R^*$ given the efficiency $\epsilon(\pi_*)$. This fact can be used to solve for $\epsilon(\pi_*)$ once we have measured $R^*$ in the data. The value that we get in our data is $R^* = 0.142 \pm 0.006(stat.) \pm 0.002(syst.)$.

### B. Tagging on $D^{**}$ Pions

Same-Side Tagging has some appealing features, but it also has one notable weakness when applied to the semi-exclusive $\ell D^{(*)}$ samples. Because of the virtual impossibility of reliably reconstructing all the $D^{**}$ states we are resigned to not even attempt to reconstruct them. This means that the charged pions from $D^{**} \to D^{(*)}\pi$ decays are lost, and give rise to the $B^0 \leftrightarrow B^+$ cross-talk. This cross talk is accounted for in the sample composition, but in addition to this effect a more insidious problem arises: it is possible that the tagging algorithm may select the $\pi_{**}$ *as the tag.* Since the $\pi_{**}$ is part of the decay chain its charge is 100% correlated with the $B$ flavor at the time of decay, this gives rise to a false dilution. The requirement that the tagging track impact parameter be within $3\sigma$ of the primary vertex suppresses $\pi_{**}$ as tags, but this cut can not eliminate all of them, especially when the $B$ vertex has only a small displacement from the primary. Although we can not reliably reconstruct $D^{**}$ decays such that we could measure how often we tag on $\pi_{**}$ tracks, we do not need to be able to do so to find out how often we tag on $\pi_{**}$ tracks. The basic idea is that we look at the distribution

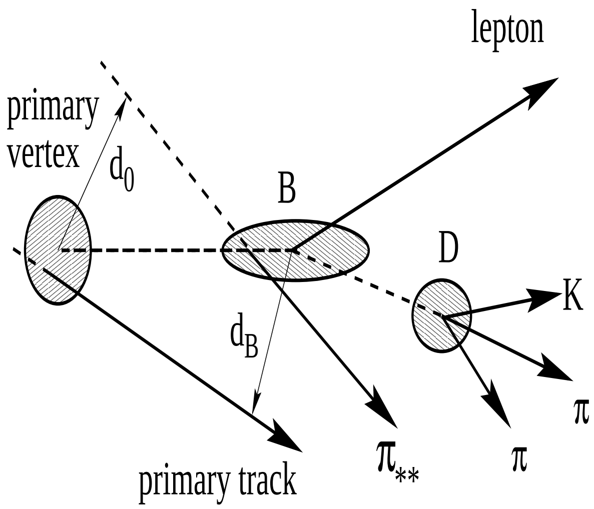


FIG. 3: A schematic representation of a $B \to \nu \ell D^{**}$ decay. SST candidate tracks originate from the primary vertex, while the $\pi^{\pm}_{**}$ track originates from the $B$ decay vertex. The impact parameter of a track with respect to the primary vertex is $d_0$ while the impact parameter with respect to the $B$ vertex is given by $d_B$. When the $B$ vertex and the primary vertex are well separated, the $\pi^{\pm}_{**}$ track usually has a large $d_0$ and a small $d_B$. The converse is true for primary tracks.

of track impact parameters *with respect to the $B$ vertex* and measure the right-sign excess for tracks near the $B$-vertex. We ascribe this excess to $\pi_{**}$ pions coming from $D^{**}$ decays.

We denote the probability to tag on a $\pi_{**}$ as $\xi(ct)$. This probability will depend upon the geometry and kinematics of the $B$ and $D^{**}$ decays, as this determines the likelihood that the $\pi_{**}$ track points to the primary vertex well enough to be considered. But it also depends upon the characteristics of the surrounding fragmentation and underlying event tracks, i.e. how much competition there is to be chosen as the track with the smallest $p_t^{\rm rel}$. We use PYTHIA Monte Carlo [5] to determine the $ct$ dependence of the $\pi_{**}$ tagging probability, as this is governed by geometry and kinematics. We do not, however, completely trust the Monte Carlo to faithfully represent the surrounding fragmentation and underlying tracks, but this uncertainty only effects the overall normalization on the tag probability, and not its $ct$ dependence. We therefore represent the $\pi_{**}$ tagging probability as:

$$\xi(ct) = \xi_{norm} \cdot \xi_{MC}(ct), \tag{2}$$

where $\xi_{norm}$ is the normalization needed to scale the simulation to agree with the data, and $\xi_{MC}(ct)$ is the shape of that distribution, which is taken from Monte Carlo simulation. Figure 4 shows the $ct$ dependence of tagging on $\pi_{**}$ tracks in Monte Carlo.

To determine the normalization, $\xi_{norm}$, we remove the $d_0/\sigma_0$ cut from the data (analogous to Figure 4, left), thereby eliminating the $ct$ dependence as well as enriching the sample in $\pi^{\pm}_{**}$ tags. We divide these "pseudo-tagged" events into right-sign and wrong-sign tags, and make the distribution of the impact parameter significances with respect to the $B$ vertex, $d_B/\sigma_B$. The difference between right-sign and wrong-sign tags, after applying a scale factor to the wrong-sign tags to be equal to the right-sign tags for large values of $d_B/\sigma_B$, is the number of $\pi_{**}$ tags in the data, as shown in Figure 5. Finally, we take the number of measured $\pi_{**}$ pseudo-tags, count total number of pseudo-tags $N(tags)$ and compute the fraction of $B$ decays where $\pi^{\pm}_{**}$ tracks are pseudo-tags,

$$R_k^{**} \equiv \frac{N(\pi_{**}^{tag})}{N(tags)}. \tag{3}$$

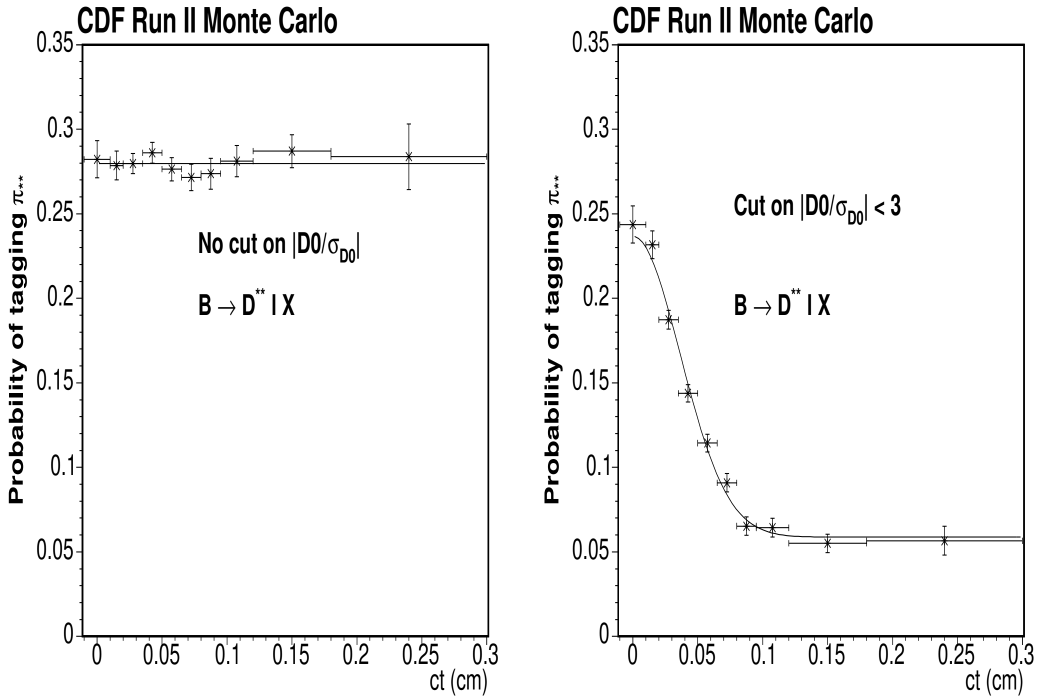


FIG. 4: The $ct$ dependence of tagging on $\pi_{**}$ tracks. The left plot is the PYTHIA result for tagging on $\pi_{**}$ tracks when they are *not* required to be consistent with the primary vertex (remove $d_0/\sigma_0 < 3.0$ cut). The right plot is the distribution of the $\pi_{**}$ tags when this cut is imposed, along with a fit of a Gaussian centered at zero plus a constant background.

## V. PROPER DECAY TIME

### A. $\mathcal{K}$-Factor Corrections

A time-dependent analysis based on the incomplete reconstruction of $B$ mesons must contend with the fact that the partial reconstruction is missing momentum, and thus the kinematic transformation of a decay distance to proper time is incomplete. The true proper time $\hat{t}$ of a $B$ decay is determined by using its projected transverse decay length relative to the primary vertex $L_{xy}(B)$, by

$$c\hat{t} = \frac{L_{xy}(B)\ m(B)}{p_T(B)}, \tag{4}$$

where $m(B)$ is the mass of the $B$ and $p_T(B)$ its transverse momentum. The canonical method for dealing with the fact that the $B$ is only partially reconstructed is to use Monte Carlo-derived average corrections $\mathcal{K}_{kh}$ relating the reconstructed parts of the transverse momentum $p_T(\ell D)$ and $L_{xy}(\ell D)$ to that of the complete $p_T(B)$ and $L_{xy}(B)$, *i.e.*,

$$\mathcal{K}_{kh} \equiv \left\langle \frac{p_T(\ell D)}{p_T(B)} \frac{L_{xy}(B)}{L_{xy}(\ell D)} \right\rangle_{MC} \tag{5}$$

for decay chain $h$ contributing to signature $k$. This gives us an average correction factor for obtaining the true proper time of the $B$ decay. The direct decay chains have mean values of ∼85%, and RMS values of ∼12%. The $\mathcal{K}$-factor distributions for the three direct decay chains are shown in Figure 6.

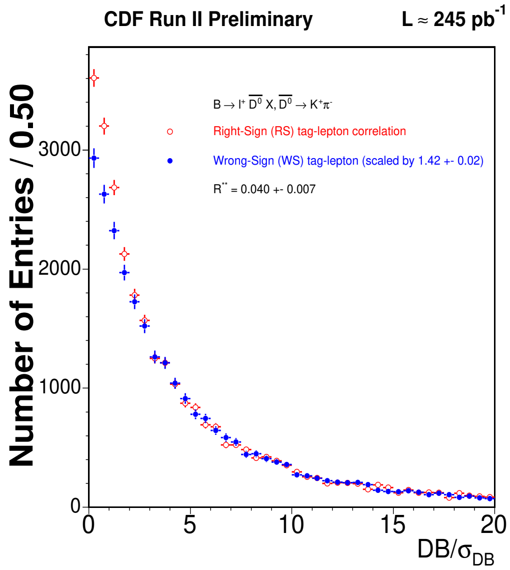


FIG. 5: $R^{**}$ determination for $B \to l^+\overline{D}^0 X(\overline{D}^0 \to K^+\pi^-)$. The plot shows right-sign contribution and the scaled wrong-sign contribution, to be equal to the right-sign contribution for large values of $d_B/\sigma_B$. The difference between both contributions is the number of $\pi_{**}$ tags in the data.

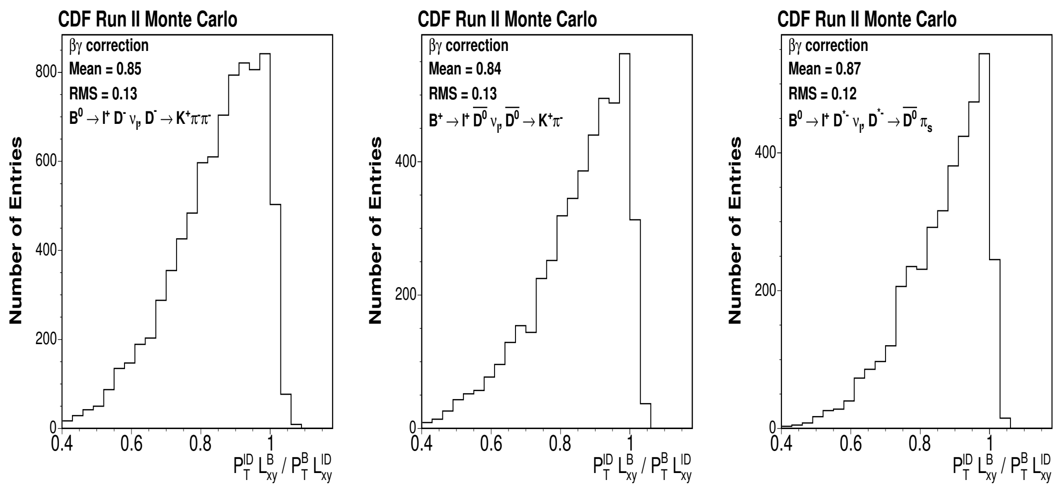


FIG. 6: The $\mathcal{K}$-factor distributions for the three direct decay chains: $D^-$ (left plot), $D^0$ (middle plot), and $D^*$ (right plot)

## B. Proper Time Resolutions

The use of $p_T(\ell D)$ rather than the true $p_T(B)$ smears the $ct$ distribution in addition to the *average* shift considered above. The difference between the reconstructed proper decay distance $ct_k^{0,+}$ and the true distance $\hat{ct}$ is

$$\Delta ct \;\equiv ct_k^{0,+} - \hat{ct} = \Delta(L_{xy}(B)/\beta_T\gamma). \tag{6}$$

The $\Delta ct$ distribution is expected to have a dependence on the reconstruction resolution via the $\Delta L_{xy}(B)$ term and an additional smearing due to our average corrections by $\Delta(1/\beta_T\gamma)$.
Approximating $1/\beta_T\gamma$ with its mean value $\langle 1/\beta_T\gamma\rangle$ gives

$$\Delta ct = \left\langle \frac{1}{\beta_T\gamma} \right\rangle \Delta L_{xy}(B) \oplus ct\frac{\Delta(1/\beta_T\gamma)}{\langle 1/\beta_T\gamma\rangle}, \tag{7}$$

Given this dependence of $\Delta ct$ on the proper time in Eq. (7), we parameterize the $ct$ resolution as

$$\sigma^{ct}(ct) = \sigma^{ct}(0) \oplus b \times ct \equiv \sqrt{(\sigma^{ct}(0))^2 + (b \times ct)^2}. \tag{8}$$

We use the RMS spread of the $\Delta ct$ distribution for bin $ct$ as the resolution $\sigma^{ct}(ct)$, and fit the RMS values of the various $ct$ bins for the slope and offset of Eq. (8).

## VI. TAGGED FLAVOR ASYMMETRY

It is straightforward to apply the SST to the $\ell D^{(*)}$ events. We classify events for each decay signature as having the "unmixed" lepton-tag charge combination (*e.g.*, $\ell^+\pi^+$ for $B^0$ mesons and $\ell^+\pi^-$ for $B^+$ mesons), or the "mixed" one with the inverted $\pi$ charge. The time integrated tagger results are shown in Table II. Efficiencies and raw asymmetries are computed using the overall time integrated mass fits. The overall weighted average efficiency is (67.3 ± 0.1 (stat.))%.

| | $B \to \ell D^0 X$ | $B \to \ell D^- X$ | $B \to \ell D^* X$ |
|---|---|---|---|
| Efficiency | 0.6684 ± 0.0018 | 0.6790 ± 0.0025 | 0.6874 ± 0.0048 |
| Raw asymmetry | 0.1900 ± 0.0051 | 0.0460 ± 0.0082 | 0.0586 ± 0.0125 |

TABLE II: Time integrated tagger results without corrections applied to the data. Efficiencies and raw asymmetries are computed using the overall time integrated mass fits. Errors are only statistical.

We split each sample in ten $ct$ bins, and the numbers of unmixed ($N_k^U(ct_{kd})$) and mixed ($N_k^M(ct_{kd})$) events for signature $k$ in the discrete $ct_{kd}$ bin are then used to compute the measured asymmetry,
The largest background source in our samples originates from missidentified leptons together with a real $D$ meson. This fraction is determined by computing the $D$ mass yields using the *wrong charged lepton and* $D$ pair combinations. Note that Righ-Sign, Wrong-Sign and Non-tagged yields are computed always using the *right charged lepton and* $D$ pairs, i.e. $\ell^+\overline{D}^0$, $\ell^+D^-$ and $\ell^+D^{*-}$. We assume that the amount of right charged lepton $D$ pair combination originating from missidentified leptons is equal the *wrong charged lepton and* $D$ pair combinations. This is not entirely obvious because charge correlations in certain decays could enhance right charge or wrong charge lepton and $D$ combinations. The fact that we observe within statistical uncertainties the same amount of missidentified leptons in right sign and wrong sign tags supports this assumption. To correct for missidentified leptons we subtract the measured number of wrong charged lepton and $D$ pair combinations from the right charged lepton and $D$ pair combinations, and compute the tagged flavor asymmetries with the such corrected yields.
The prediction for the measured asymmetry is given by,

$$\begin{aligned} \overline{\mathcal{A}}_k &= \{\mathcal{F}_k^0 - \xi\mathcal{F}_k^{0,**}\}\mathcal{A}^0 + \xi\mathcal{F}_k^{0,**}\{-1\} \\ &+ \{\mathcal{F}_k^+ - \xi\mathcal{F}_k^{+,**}\}\{-\mathcal{A}^+\} + \xi\mathcal{F}_k^{+,**}\{+1\} \\ &+ \mathcal{F}_k^{Bck}\overline{\mathcal{A}}_k^{Bck}, \end{aligned} \tag{9}$$

where $\mathcal{A}^0$ and $\mathcal{A}^+$ are the true asymmetries for $B^0$ and $B^+$, $\mathcal{F}_k^0$ and $\mathcal{F}_k^+$ are the fractions for $B^0$ and $B^+$, $\mathcal{F}_k^{0,**}$ and $\mathcal{F}_k^{+,**}$ are the fractions of $\pi^{\pm}_{**}$ tags coming from $B^0$ and $B^+$ decays, the $-1$ $(+1)$

| Decay / Channel | $B \to \ell D^* X$ | $B \to \ell D^- X$ | $B \to \ell D^0 X$ |
|---|---|---|---|
| $B_s \to \nu\ell D_s^{(*)} X,\ D_s \to K^* K$ | 0.0 | 3.2 | 0.0 |
| $B \to D_s^{(*)} D^{(*)} X,\ D_s^{(*)} \to \ell X$ | 1.1 | 2.6 | 1.5 |
| $B_s \to \nu\ell D_s^{**} X,\ D_s^{**} \to DK$ | 0.0 | 0.0 | 1.9 |
| $B_s \to \nu\ell D_s^{**} X,\ D_s^{**} \to DK^0$ | 0.3 | 0.7 | 0.4 |
| $B \to D^{(*)} D^{(*)} K$ | 1.4 | 0.7 | 0.9 |
| $B \to \nu\tau D^{(*)} X$ | 1.9 | 2.0 | 1.6 |
| Total | 4.8 | 9.3 | 6.3 |

TABLE III: Fraction (in %) of physics background events for each decay channel with respect to the number of signal events.

asymmetry factors in the second (fourth) term reflect the perfect correlation of $\pi^{\pm}_{**}$ tags, $\xi$ is the fraction of $\pi^{\pm}_{**}$ tracks selected as tags. Finally, $\mathcal{F}_k^{Bck}$ and $\mathcal{A}_k^{Bck}$ is the fraction and the asymmetry factor corresponding to some physics backgrounds respectively. They are real physics processes with the correct correlation between the lepton and the $D$ meson. The fraction of physics background events for each decay channel with respect to the number of signal events is shown in Table III.

## VII. FLAVOR ASYMMETRY FIT

### A. The $\chi^2$ function

We form a $\chi^2$ function to simultaneously fit $\Delta m_d$, $\mathcal{D}_+$, and $\mathcal{D}_0$ over all $ct$ bins of all decay signatures by comparing the predictions $\overline{\mathcal{A}}_k(ct_{kd})$ against the measured asymmetries $\mathcal{A}_k^{(meas)}(ct_{kd})$, where $ct_{kd}$ is used for $\mathcal{A}_k^{(meas)}$ since we were restricted to the direct chain $ct_{kd}$ when binning the data. The $\overline{\mathcal{A}}_k(ct_{kd})$ asymmetry depends not only upon the parameters $\Delta m_d$, $\mathcal{D}_0$, and $\mathcal{D}_+$, which are of direct interest, but also on $\tau_0$, $\tau_+/\tau_0$, $R_f$ $(\equiv f^*/f)$, $f^{**}$, $P_V$, $\epsilon(\pi_*)$, and $\xi_{norm}$ through the $\mathcal{F}^{0,+}$ fractions. The last two parameters are also expressed as functions of $R^*$ and $R_k^{**}$, as well as the other composition parameters. Then, the $\chi^2$ function is given by,

$$\chi^2 = \sum_{ct\text{bins},k} \left(\frac{A_k^{meas}(ct) - A_k^{fit}(ct)}{\sigma_A^{meas}}\right)^2 + \sum_k \left(\frac{R_k^{**meas} - R_k^{**fit}}{\sigma_{R_k}^{**meas}}\right)^2 + \left(\frac{R^{*meas} - \epsilon(\pi_s)^{fit} R^*}{\sigma_{R^*}^{meas}}\right)^2 +$$
$$\left(\frac{f^{**PDG} - f^{**}}{\sigma_{f^{**}}^{PDG}}\right)^2 + \left(\frac{R_f^{PDG} - R_f}{\sigma_{R_f}^{PDG}}\right)^2 + \left(\frac{(\tau_{B^+}/\tau_{B^0})^{PDG} - (\tau_{B^+}/\tau_{B^0})}{\sigma_{(\tau_{B^+}/\tau_{B^0})}^{PDG}}\right)^2 + \left(\frac{(\tau_{B^0})^{PDG} - (\tau_{B^0})}{\sigma_{(\tau_{B^0})}^{PDG}}\right)^2$$

### B. Result of the Fit

The $\chi^2$ function is minimized over ten $ct$ bins for all three decay signatures simultaneously, letting the unknown parameters float freely, and the known inputs to vary within their errors. The asymmetry data and fit results are shown in Figure 7, and listed in Table IV.

The $\Delta m$ value is in good agreement with the PDG, $\Delta m = 0.443 \pm 0.060\ ps^{-1}$. The dilutions are $(12.9 \pm 1.9)\%$ and $(28.2 \pm 1.7)\%$ for the neutral and charged mesons. We get a value of $\epsilon(\pi_*) = (51.7 \pm 3.3)\%$, which agrees pretty well with the expected value from Monte Carlo, 55%. In addition $\xi_{norm}$, the normalization factor to agree the simulation with the data the probability of tagging a $\pi_{**}$ is close to one, which means the Monte Carlo describes rather well the data.

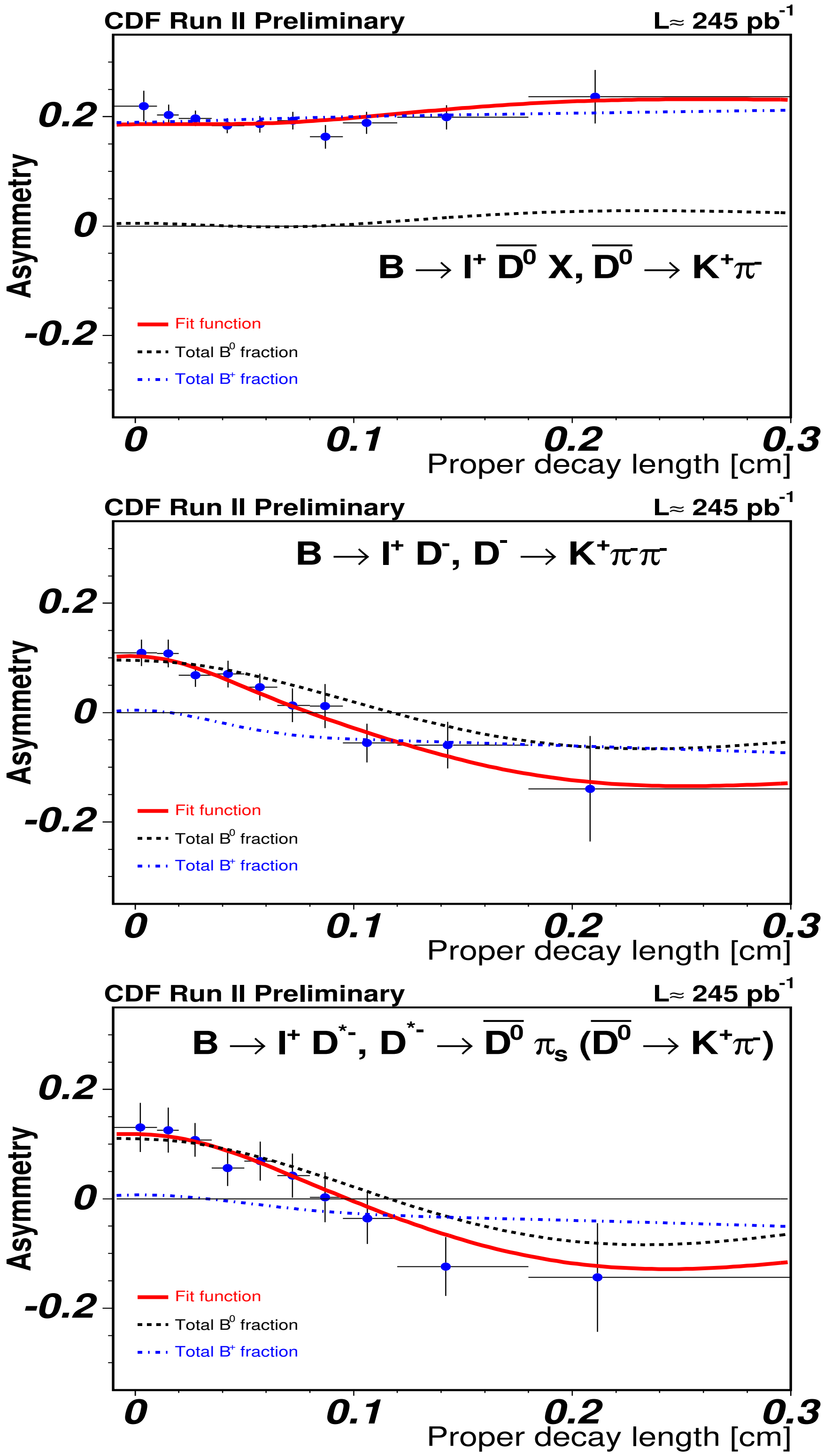


FIG. 7: Plots of the measured asymmetries with the fit results superimposed (red color). The separate contributions of $B^0$ (black color) and $B^+$ (blue color) decays to each signature are also shown.

| Parameter Name | Init. Value | Constraint Error | Final Value |
|---|---|---|---|
| $\Delta m_d$ | — | — | $0.4428 \pm 0.0602$ |
| $D_0$ | — | — | $0.1279 \pm 0.0186$ |
| $D_+$ | — | — | $0.2830 \pm 0.0167$ |
| $R_f$ | 2.1800 | 0.1400 | $2.1451 \pm 0.1400$ |
| $f^{**}$ | 0.3100 | 0.0500 | $0.2997 \pm 0.0452$ |
| $P_V$ | — | — | $0.4649 \pm 0.1424$ |
| $\epsilon(\pi_*)$ | — | — | $0.5164 \pm 0.0326$ |
| $\xi_{norm}$ | — | — | $1.1702 \pm 0.2176$ |
| $\tau_0$ | 0.0461 | 0.0004 | $0.0461 \pm 0.0004$ |
| $\tau_+/\tau_0$ | 1.0860 | 0.0170 | $1.0806 \pm 0.0170$ |

TABLE IV: Results of the full $\chi^2$ fit along with the initial values. Parameters which are constrained in the $\chi^2$ fit to their initial value also have an "error" by which they are constrained.

## VIII. SYSTEMATICS UNCERTAINTIES

Separation of systematic and statistical errors in the $B^0$ mixing measurement is performed for semileptonic $B$ decays. Due to the complex sample composition of the semi-exclusively reconstructed $\ell D^{(*)}$ candidates additional external measurements become important in the $B^0$ mixing analysis. We describe the separation of the errors from the statistical power of our data from the effect of the external constraints used in the final fit.

When we perform the $B^0$ mixing measurement the complicated sample composition becomes an important effect. In particular the higher resonances, referred to as $D^{**}$, which are never reconstructed for this analysis can not be determined in this fit. Therefore external constraints are necessary. To evaluate the statistical power of our data is interesting to separate the effect of the constraints on our measurement from the total uncertainties. We use a simple linearization of the fit solution to describe the data. Through the linearization it becomes straightforward to extract the influence of the external constraints, taking into account the correlations among the several parameters in the fit.

Other systematic uncertainties on the extracted dilutions and oscillation frequency derive from several sources: uncertainties due to the $b$-quark and $B$ decay models used in the simulation; the $L_{xy}$ resolution, which affects the $ct$ computations; the measurements of $R^*$ and $R^{**}$; the shape of $\xi_{MC}(ct)$ taken from the Monte Carlo simulation; the different background contributions; and the lifetime of the $B$ mesons.

Systematic uncertainties from all sources are listed in Table V. By far the biggest contribution comes from the uncertainties on the sample composition parameters. The combined systematic uncertainty is still smaller than the statistical error in the case of $\Delta m_d$, and both contributions are comparable in the case of the dilutions measurements.

## IX. SUMMARY

We have reconstructed $B \to \ell D^{(*)}$ candidates from 245 pb$^{-1}$ of Run II data, and flavor tagged the events with the same-side algorithm. We observe the time-dependent flavor oscillation for the $B^0$, and measure the oscillation frequency to be

$$\Delta m_d = (0.443 \pm 0.052\ (stat.) \pm 0.030\ (s.c.) \pm 0.012\ (syst.))ps^{-1}, \tag{10}$$

and the tagging dilutions are

$$D_0 = (12.8 \pm 1.6\ (stat.) \pm 1.0\ (s.c.) \pm 0.6\ (syst.))\%,$$
$$D_+ = (28.3 \pm 1.3\ (stat.) \pm 1.1\ (s.c.) \pm 1.0\ (syst.))\%.$$

| Error Source | $\Delta m_d$ ($ps^{-1}$) | $D_0$ (%) | $D_+$ (%) |
|---|---|---|---|
| Sample composition | 0.0303 | 1.01 | 1.09 |
| $b$-quark model | 0.0048 | 0.23 | 0.41 |
| $B$ decay model | 0.0079 | 0.31 | 0.09 |
| $L_{xy}$ resolution | 0.0016 | 0.01 | 0.01 |
| $R^{*/**}$ measurements | 0.0039 | 0.16 | 0.25 |
| $\xi_{MC}(ct)$ shape | 0.0047 | 0.25 | 0.13 |
| Fitting mass | 0.0023 | 0.01 | 0.05 |
| $B \to DX$ background | 0.0022 | 0.32 | 0.77 |
| $c\bar{c}$ gluon splitting | 0.0008 | 0.24 | 0.33 |
| $B$ Lifetime | 0.0005 | 0.01 | 0.03 |
| Total, except sample composition | 0.0117 | 0.63 | 0.98 |
| Total | 0.0325 | 1.19 | 1.47 |

TABLE V: Table of systematic uncertainties.

Therefore, the same side tagging effectiveness are

$$\epsilon D^2\ (B^0) = (1.1 \pm 0.3\ (stat.) \pm 0.2\ (s.c.) \pm 0.1\ (syst.))\%,$$
$$\epsilon D^2\ (B^+) = (5.3 \pm 0.5\ (stat.) \pm 0.4\ (s.c.) \pm 0.4\ (syst.))\%.$$

### Acknowledgments

We thank the Fermilab staff and the technical staffs of the participating institutions for their vital contributions. This work was supported by the U.S. Department of Energy and National Science Foundation; the Italian Istituto Nazionale di Fisica Nucleare; the Ministry of Education, Culture, Sports, Science and Technology of Japan; the Natural Sciences and Engineering Research Council of Canada; the National Science Council of the Republic of China; the Swiss National Science Foundation; the A.P. Sloan Foundation; the Bundesministerium fuer Bildung und Forschung, Germany; the Korean Science and Engineering Foundation and the Korean Research Foundation; the Particle Physics and Astronomy Research Council and the Royal Society, UK; the Russian Foundation for Basic Research; the Comisión Interministerial de Ciencia y Tecnología, Spain; and in part by the European Community's Human Potential Programme under contract HPRN-CT-20002, Probe for New Physics.

[1] CDF Collaboration, F. Abe *et al.*, Phys. Rev. Lett. **80**, 2057 (1998), Phys. Rev. D**59**, 032001 (1999); and P. Maksimovic, PhD dissertation, MIT, 1998 (a.k.a. CDF 4614).

[2] F. Abe, et al., Nucl. Instrum. Methods Phys. Res. A **271**, 387 (1988); D. Amidei, et al., Nucl. Instum. Methods Phys. Res. A **350**, 73 (1994); F. Abe, et al., Phys. Rev. D **52**, 4784 (1995); P. Azzi, et al., Nucl. Instrum. Methods Phys. Res. A **360**, 137 (1995); The CDFII Detector Technical Design Report, Fermilab-Pub-96/390-E.

[3] K. Hagiwara *et al.*, Physical Review **D66**, 010001 (2002).

[4] CDF Collaboration, F. Abe *et al.*, Phys. Rev. Lett. **81**, 5513 (1998), T. Affolder *et al.*, Phys. Rev. D**61**, 072005 (2000); and K. Kelley, PhD dissertation, MIT, 1999 (a.k.a. CDF 4767).

[5] T. Sjostrand et al., High-Energy-Physics Event Generation with PYTHIA 6.1, Comput. Phys. Commun. **135**, 238 (2001).